Mechanophotopatterning on a Photoresponsive Elastomer

*Christopher J. Kloxin, Timothy F. Scott, Hee Young Park, and Christopher N. Bowman**

The fabrication of well-defined topographical features or textures is a dynamic area of research owing to their extraordinary potential in applications ranging from complex optics to tunable and responsive surfaces.[1–6] Here, mechanophotopatterning (MPP) on a photoresponsive elastomer is introduced and enables for the first time the ability to precisely and simultaneously manipulate both material shape and surface topography by exposure to light without the need for solvents, molding, or physical contact. MPP is a unique patterning approach whereby deformation is applied to an elastomeric material capable of photoinduced structural modification to alter its equilibrium geometry, elegantly complementing previous mechanically assisted patterning techniques.[7–9] This material responds to MPP by continuously and locally deforming via polymer network connectivity rearrangement, which enables 3D control of its geometry. Unlike conventional photolithographic approaches, MPP forgoes any wet chemistry or surface deposition/modification processing and simplifies multi-tiered feature fabrication. Furthermore, in contrast with mechanically assisted patterning techniques that utilize buckling phenomena,[4,8,9] MPP on a photoresponsive elastomer allows an arbitrary-sized and designed feature to be written into the material multiple times, while also being able to change the overall shape of the material.

Photoinduced structural adaptation in elastomeric networks is effected by incorporating functional groups capable of altering network connectivity upon irradiation. In this work, addition–fragmentation chain transfer (AFCT)-capable functional groups are incorporated in the backbone of an elastomeric covalent adaptable network.[10] This AFCT-capable elastomeric network is fabricated by utilizing a base-catalyzed Michael-type "click" reaction[11,12] between thiol and acrylate monomers (**Figure 1**a), proceeding quantitatively via a rapid, non-radical mechanism. Upon photomediated radical generation, interstrand AFCT through the allyl sulfide functional groups incorporated in the network backbone results in network connectivity rearrangement (Figure 1b), effecting photoinduced plasticity and providing a facile route for stress relaxation and equilibrium geometry modification.[13,14] The latent photoinitiator, incorporated into the initial resin formulation, generates radicals by homolytic photolysis to initiate the AFCT-mediated network rearrangement. The decoupling of polymer synthesis from subsequent network rearrangement ensures that the radical yielding photoinitiator is not consumed during network fabrication. A particularly notable characteristic of the AFCT-capable elastomer is its extraordinary propensity for photoinduced stress relaxation. As shown in Figure 1c, irradiation of an optically thin sample achieves unprecedented, nearly complete stress relaxation (i.e., ≈99% permanent set)[15] with no concomitant degradation of the crosslinked polymer network structure. The new equilibrium shape of the material corresponds to the applied strain, and the thickness is reduced (i.e., via the Poisson effect) in a predictive manner, assuming only volume conservation.

A simple illustration of MPP is readily demonstrated via irradiation of an optically thin AFCT-capable elastomer under uniaxial strain (see **Figure 2**). Here, a sample is uniaxially strained and irradiated through a photomask to project a hexagonal array onto the sample (Figure 2a). The irradiated regions undergo photoinduced plasticity, resulting in a permanent set of the new shape. As shown in Figure 2b, the resultant material exhibits a well-defined hexagonal pattern commensurate with the mask. In contrast to other mechanically assisted patterning methods, where patterns are formed via a buckling phenomenon,[4,8,9] the lateral size-scale of the features is strictly controlled by the mask design. The width contraction at the middle of the sample is a result of the uniaxial extension, the geometry of which becomes the new equilibrium shape upon complete photoinduced stress relaxation. Further examination of the surface topography (Figure 2c) reveals a hexagonal array of troughs that corresponds to the projected hexagonal pattern in both shape and dimension. MPP is observed to yield rounded features that are often difficult to produce using conventional photolithography (Figure 2c), which are particularly useful for the fabrication of more complex geometries such as that of a lens. These rounded features are an artifact of the progressive change in light exposure of the material as it moves from an irradiated to an unirradiated region. This localized plastic flow yields rounded features, as observed, which are deterministically defined by the combined strain and incident irradiation. Despite the physical displacement of material, the topographic periodicity exhibits excellent fidelity with the photomask periodicity.

Although there are several patterns achievable by 1D extension, the fabrication of more complex patterns requires multidimensional mechanical strain. For example, an irradiated line parallel to the applied deformation has reduced line sharpness when compared with a line that is perpendicular to this deformation. In principle, a uniaxially stretched sample could simply be rotated 90° followed by another stretching and irradiation step. This approach requires two masks that are specifically designed to account for the extension as well as giving consideration to the amount of photoinitiator remaining after the first irradiation. A convenient alternative is to stretch the material simultaneously in two dimensions prior to and throughout patterning. To demonstrate this concept, a sample was stretched

Prof. C. J. Kloxin, Prof. T. F. Scott, H. Y. Park, Prof. C. N. Bowman
University of Colorado
Department of Chemical and Biological Engineering
424 UCB, ECCH 111
1111 Engineering Dr., Boulder, CO 80309–0424, USA
E-mail: christopher.bowman@colorado.edu

DOI: 10.1002/adma.201100323

ADVANCED MATERIALS
www.advmat.de

www.MaterialsViews.com

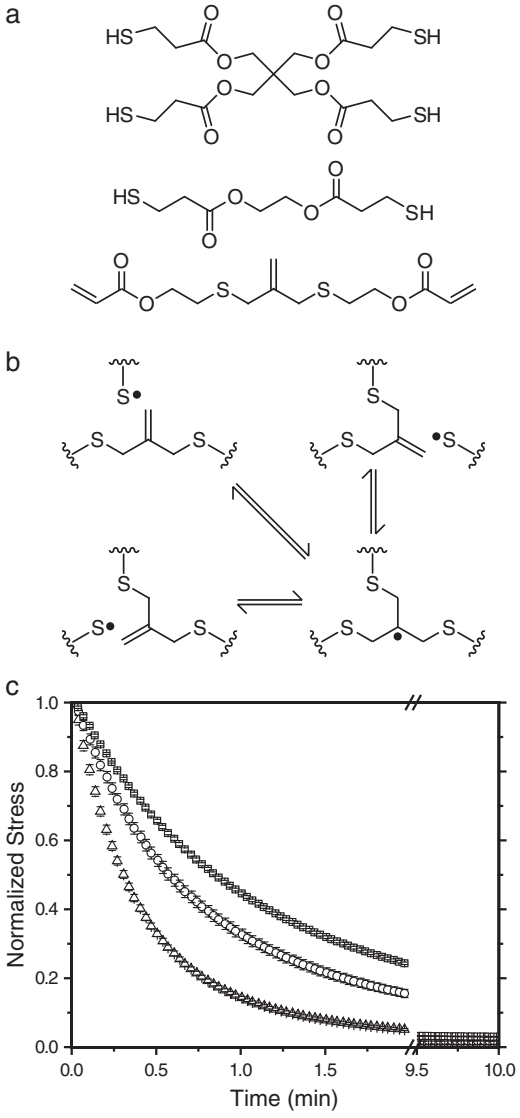

Figure 1. Photoresponsive formulation and stress relaxation properties. a) The resins were formulated with a 1:3 mixture of pentaerythritol tetrakis(3-mercaptopropionate) (PETMP–top) and ethylene glycol bis(3-mercaptopropionate) (EGBMP–middle) and a stoichiometric balance of 2-methylene-propane-1,3-bis(thioethyl acrylate) (MBTA–bottom–i.e., where the thiol to acrylate functional group ratio was 1:1) to produce a network possessing a Young's modulus of ≈0.71 MPa. The MBTA component incorporates allyl sulfide functional groups into the network strands. b) The allyl sulfide group facilitates bond rearrangement via radical mediated AFCT.[14] c) Photoinduced stress relaxation (normalized), owing to the AFCT mechanism, for 5 mW cm^{-2} (squares), 10 mW cm^{-2} (circles), and 20 mW cm^{-2} (triangles) at 405 nm light, which exhibit 96, 98, and >99% permanent set after 10 min of irradiation.

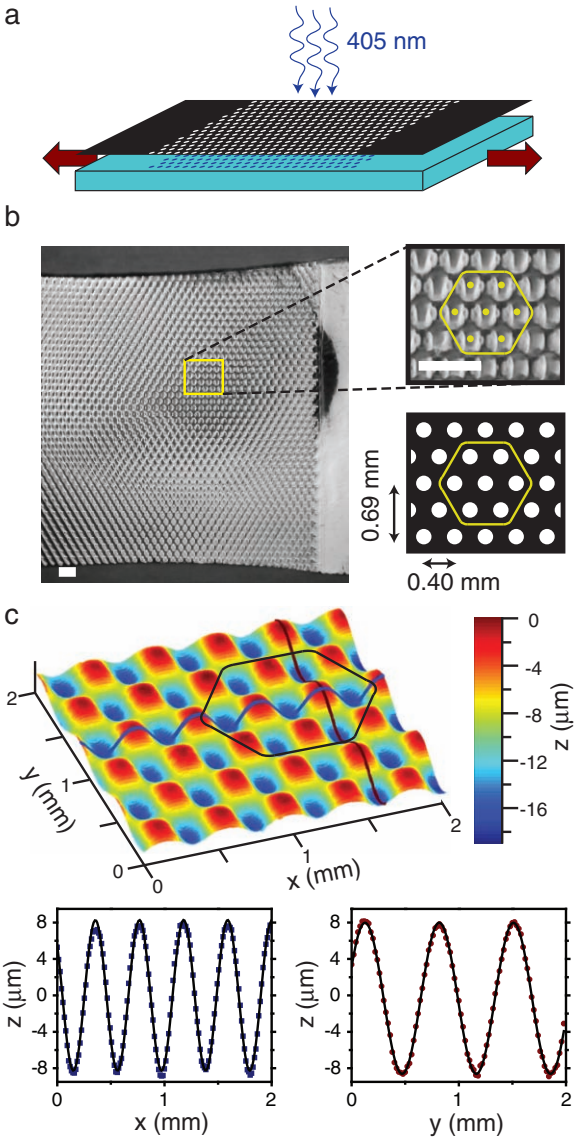

Figure 2. Mechanophotopatterning of a uniaxially deformed sample. a) The material is stretched to 20% strain and irradiated at 405 nm (10 mW cm^{-2} for 5 min) though a hexagonal patterned film transparency (0.2-mm-diameter circles separated by 0.2 mm). b) After irradiation, the material exhibits the hexagonal pattern, consistent with the pattern of the mask (scale bar = 1 mm). c) Stylus profilometry reveals an excellent correspondence between the mask and the topographical features on the surface of the sample. The periodicities are 0.69 and 0.41 along the *y*- and *x*-axis, respectively, where markers are experimental data and lines are sinusoidal fits.

10% in two dimensions and irradiated through a mask of concentric rings (**Figure 3**a). The sample was subsequently flood irradiated (i.e., without a mask) to eliminate any residual stress. Unlike the previous uniaxially stretched sample, the spatial pattern fidelity is not precisely preserved. The diameter of the inner ring is identical to that of the mask (1.4 mm); however, the rings further from the center become progressively larger than that of the mask (9.7 mm vs 9.4 mm for the largest ring). This distortion illustrates a distinct characteristic of the MPP approach. In the deformed state, each unit volume within the material exerts an equivalent force. Upon photoexposure, the irradiated volume undergoes plastic flow driven by a force imbalance with the unirradiated volume that, for the current case, includes the region beyond the boundary of the outermost ring. Since the unirradiated volumes between features are not equivalent to that beyond the outer boundary, there exists a plastic flow bias in the radial direction responsible for

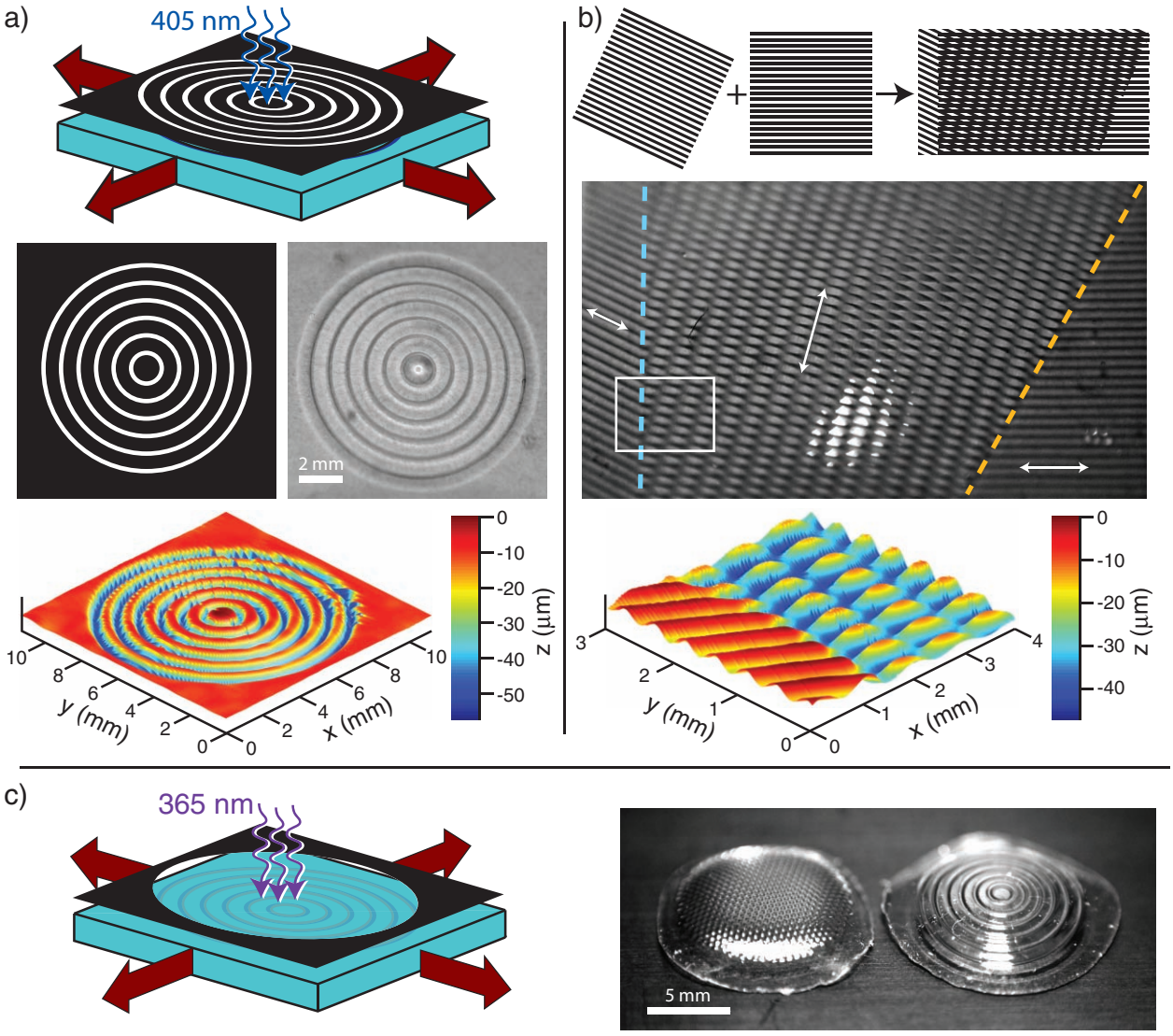

Figure 3. Mechanophotopatterning of 2D deformed samples. a) The material is stretched to 10% strain along two perpendicular axes and irradiated at 405 nm (10 mW cm^{-2} for 5 min) through a concentric ring mask (0.4-mm-thick lines, separated by 1.2 mm). The sample was subsequently flood irradiated (no mask using 405 nm at 10 mW cm^{-2} for 5 min) to eliminate residual stress. The image compares favorably with the pattern of the mask. Stylus profilometry reveals that the rings are radially symmetrical, with the larger rings having slightly larger diameters (trough-to-trough) than that of the mask (9.7, 8.1, 6.4, 4.8, 3.1, and 1.4 mm vs 9.4, 7.8, 6.2, 4.6, 3.0, and 1.4 mm, respectively). b) The sample is placed under the same strain as in (a); however, the sample is first irradiated through horizontal lines (405 nm at 10 mW cm^{-2} for 45 s through 0.2 mm lines), followed by rotating the mask 30° and reirradiated (405 nm at 10 mW cm^{-2} for 5 min). The mask pattern and their sum are shown, which compares favorably to the image shown (arrows indicate the direction of pattern–the box dimensions, 3×4 mm^2, are the same as the profilometry shown below). Stylus profilometry of the sample reveals that the fidelity of the mask periodicity is preserved and that the doubly exposed region has troughs that are approximately twice that of the singly exposed region. c) Using the same irradiation protocol as in (a) except the sample was subsequently exposed to UV irradiation (365 nm at 1 mW cm^{-2} for 30 s), which resulted in the warped samples shown (left and right samples were initially irradiated with the hexagonal array and concentric rings masks, respectively).

the distortion. Control over this phenomenon is readily accomplished via mask design and provides even greater command over the trough depth and profile.

The facile production of complex topographical features of varying depths can be achieved by sequential exposures. An illustration of this unique capacity of MPP is shown in Figure 3b. Here, the material is stretched 10% in two dimensions and irradiated through a mask, yielding a periodic lined pattern (right side of image, Figure 3b). The sample is subsequently reirradiated through the mask rotated 30°, again yielding a periodic lined pattern (left side of image, Figure 3b). Additionally, a third moiré pattern emerges as periodic, parallel lines rotated by 105° within the overlapped region (see Figure 3b). As anticipated, the topography reveals that the troughs in this region are approximately twice that of a single exposed region. Conversely, the regions that are unexposed after both irradiation steps do not experience photoplasticity and thus both the singly and doubly patterned regions have approximately the

same peak height. Depending on the continued radical generation capacity, multiple exposure MPP affords the ability to fabricate multi-tiered topographical features using elementary irradiation schemes.

The utilization of a non-photoinitiated polymerization approach to form the initial polymer network allows the fabrication of AFCT-capable elastomers that contain multiple radical generating species photoinitiated at different wavelengths of light. The data presented above were all collected on samples formulated to be optically thin at 405 nm with less than 40% light attenuation throughout the sample, yielding uniform photoplasticity through the sample thickness. Thus, the features are present on both the top and bottom surfaces. However, MPP can also be performed on samples formulated to be optically thick which results in the generation of a stress relaxation gradient upon irradiation, leading to controlled warping of the sample in the direction of the light propagation.[14] These two phenomena can be exploited to complement each other using multiples wavelengths to access different photoplastic outcomes, from surface topography to warping. Here, we demonstrate this capability by fabricating a material that is optically thin and thick at 405 and 365 nm, respectively, via the incorporation of both visible and UV light photoinitiators as well as a UV absorber. By patterning a two-dimensionally strained sample with 405 nm light (i.e., optically thin) and subsequently flood irradiated with 365 nm light (i.e., optically thick), the sample retains the initial surface pattern while also achieving significant surface curvature (Figure 3c). It should be noted that the sample shown in Figure 3c exhibits an artifact of the applied strain. The 2D stretching produces non-uniform off-axis strain that is most dominate at the corners of the sample (i.e., along the 45 and 135° axes) and that can be compensated for by changing the irradiation profile across the sample (via mask design) or by equibiaxial stretching. Nevertheless, by simply patterning and selecting the wavelength of light, controlled photoplasticity via the MPP approach can lead to a vast number of topological states.

Application of the MPP technique to an AFCT-capable elastomeric network provides an elegant approach to create complex topographical features and shapes. Once the network is fabricated, the final shape of the blank material is readily manipulated, requiring no wet chemistry. Moreover, the MPP process can be repeated on the same sample to produce multi-tiered or overlapped features, yielding an entirely new pattern. Constitutive modeling of this process will provide insight into mask design and irradiation conditions, leading to the precise control over the final shape and structure.[16] Beyond the direct writing of topographical features, confining the MPP process to a fine surface layer (e.g., by incorporating significant amounts of UV absorber) has further potential to instigate local instabilities, resulting in wrinkling or buckling.[1,4,7] Unlike oxidative plasma treatment of PDMS-based elastomers, surface wrinkling is readily patterned via MPP owing to the ease of light manipulation. Moreover, stressed regions within the material volume could be relaxed using focused laser light or holographic patterning. Finally, as this thiol-ene-based elastomer is readily functionalized,[17] surface modification could be performed under strain and the functional group density could be controlled by the MPP process to create surfaces with patterned polymer brush behavior[18,19] or superhydrophobicity.[20] In general, our approach for fabricating ACFT-capable networks using non-radical-based click chemistry is well-suited for a wide range of chemical modification strategies, making MPP a versatile technique for facile control over shape and surface topography in an array of advanced materials applications.

Experimental Section

Materials: 3-Chloro-2-chloromethyl-1-propene was purchased from Secant Chemical, Inc. 2-Mercaptoethanol (99%) and triethylamine (>99%) were purchased from Fisher Scientific. Acryloyl chloride (96%) was purchased from Alfa Aesar. Sodium metal (99%) and ethylene glycol dimercaptopropoinate (EGDMP, middle structure in Figure 1) were purchased from Sigma-Aldrich. Pentaerythritol tetrakis(3-mercaptopropionate) (PETMP, top structure in Figure 1) was obtained from Evans Chemetics. Irgacure 651 (2,2-Dimethoxy-2-phenylacetophenone–DMPA), Irgacure 819 (Bis(2,4,6-trimethylbenzoyl)-phenylphosphineoxide–BPO), Tinuvin 328 (2-(2H-benzotriazol-2-yl)-4,6-ditertpentylphenol) were obtained from BASF (formally Ciba) and were used without further purification.

Synthesis of 2-Methylene-Propane-1,3-Bis(2-Hydroxythioethane) (MBH): 42 g (33.8 mmol) of 3-chloro-2-chloromethyl-1-propene was added to refluxing 57.8 g (74 mmol) 2-mercaptoethanol solution of sodium methoxide (19 g sodium in 600 mL methanol). After 12 h of reflux, the salt by-product was filtered off, the solvent was evaporated, and the resulting crude product was extracted (ether/water). The ether extract was dried over calcium chloride and the solvent was subsequently evaporated to yield a slightly yellow oil. The oil was further purified using vacuum distillation (100 °C, 1.2 mm Hg). ^{1}H NMR (500 MHz, $CDCl_3$) δ: 5.04 (s, 2H), 3.73 (q, J = 6.0, 4H), 3.32 (s, 4H), 2.66 (t, J = 5.9, 4H), 2.08 (t, J = 6.2, 2H).

Synthesis of 2-Methylene-Propane-1,3-Bis(Thioethyl acrylate) (MBTA): 34 g (37.8 mmol) of acryloyl chloride in 50 mL of dichloromethane were added dropwise to a stirring solution of 38 g (27.7 mmol) triethylamine and 37 g (17.8 mmol) MBH in 450 mL of dichloromethane at 0 °C for 2 h under nitrogen protection. The solution was stirred for overnight at room temperature. The material was extracted using dichloromethane and water. The dichloromethane layer was dried using calcium chloride and then evaporated to yield a yellowish crude product. Further purification was performed using column chromatography (hexane:ethyl acetate 7:3) to obtain a clear and colorless oil. ^{1}H NMR (500 MHz, CDCl3) δ: 6.43 (dd, J = 1.4, 17.3, 2H), 6.13 (dd, J = 10.4, 17.3, 2H), 5.86 (dd, J = 1.4, 10.4, 2H), 5.06 (s, 2H), 4.29 (t, J = 6.9, 4H), 3.34 (s, 4H), 2.70 (t, J = 6.9, 4H).

Network Fabrication: The networks were formulated with 1.0 wt% Irgacure 819, 2.0 wt% Irgacure 651, and 0.5 wt% Tinuvin 328 in a 1:3 mixture of PETMP and EGDMP and a stoichiometric balance of MBTA (i.e., where the thiol to acrylate functional group ratio was 1:1). The 1:3 ratio of PETMP to EGDMP was selected to obtain a network capable of undergoing large strains. Soon after formulation (within 10 min), a catalytic amount of triethylamine (≈0.15 g) was added to approximately 1.5 g of the mixture while vortexing and then immediately sandwiched between two glass slides separated by 0.3-mm polyester shims. The samples were allowed to cure overnight and IR spectroscopy was used to confirm the complete consumption of thiol and acrylate (see Supporting Information) functional groups.

Mechanophotopatterning: The apparatus used to stretch the samples consists of a simple manually controlled micrometer linear stages attached to an optical bread board (see Supporting Information). Once the sample was stretched, the mask was mounted over the sample (≈0.2 mm from the surface) and irradiated. The light from the Hg lamp was directed to the sample through a liquid light guide equipped with a collimating lens and notch filter (centered at 405 and 365 nm, depending on the experiment). The intensity at the location of the sample was measured using a radiometer equipped with a GaAsP detector. Surface

topography of the patterned samples was determined using stylus profilometry (Dektak 200VSi stylus profilometer–Veeco).

Supporting Information

Supporting Information is available from the Wiley Online Library or from the author.

Acknowledgements

The authors acknowledge funding from the National Science Foundation Grant CBET 0933828 and National Institutes of Health, NIDCR DE 10959.

Received: January 25, 2011
Published online: March 1, 2011

[1] N. Bowden, S. Brittain, A. G. Evans, J. W. Hutchinson, G. M. Whitesides, *Nature* **1998**, *393*, 146.
[2] E. P. Chan, A. J. Crosby, *Adv. Mater.* **2006**, *18*, 3238.
[3] E. P. Chan, E. J. Smith, R. C. Hayward, A. J. Crosby, *Adv. Mater.* **2008**, *20*, 711.
[4] J. Genzer, J. Groenewold, *Soft Matter* **2006**, *2*, 310.
[5] H. Q. Jiang, D. Y. Khang, J. Z. Song, Y. G. Sun, Y. G. Huang, J. A. Rogers, *Proc. Natl. Acad. Sci. USA* **2007**, *104*, 15607.
[6] C. M. Stafford, C. Harrison, K. L. Beers, A. Karim, E. J. Amis, M. R. Vanlandingham, H. C. Kim, W. Volksen, R. D. Miller, E. E. Simonyi, *Nat. Mater.* **2004**, *3*, 545.
[7] K. Efimenko, M. Rackaitis, E. Manias, A. Vaziri, L. Mahadevan, J. Genzer, *Nat. Mater.* **2005**, *4*, 293.
[8] P. C. Lin, S. Yang, *Appl. Phys. Lett.* **2007**, *90*, 241903.
[9] D. Chandra, S. Yang, P. C. Lin, *Appl. Phys. Lett.* **2007**, *91*, 251912.
[10] C. J. Kloxin, T. F. Scott, B. J. Adzima, C. N. Bowman, *Macromolecules* **2010**, *43*, 2643.
[11] C. E. Hoyle, C. N. Bowman, *Angew. Chem. Int. Ed.* **2010**, *49*, 1540.
[12] C. E. Hoyle, A. B. Lowe, C. N. Bowman, *Chem. Soc. Rev.* **2010**, *39*, 1355.
[13] T. F. Scott, R. B. Draughon, C. N. Bowman, *Adv. Mater.* **2006**, *18*, 2128.
[14] T. F. Scott, A. D. Schneider, W. D. Cook, C. N. Bowman, *Science* **2005**, *308*, 1615.
[15] R. D. Andrews, A. V. Tobolsky, E. E. Hanson, *J. Appl. Phys.* **1946**, *17*, 352.
[16] K. N. Long, T. F. Scott, H. J. Qi, C. N. Bowman, M. L. Dunn, *J. Mech. Phys. Solids* **2009**, *57*, 1103.
[17] V. S. Khire, Y. Yi, N. A. Clark, C. N. Bowman, *Adv. Mater.* **2008**, *20*, 3308.
[18] S. T. Milner, *Science* **1991**, *251*, 905.
[19] T. Wu, K. Efimenko, J. Genzer, *J. Am. Chem. Soc.* **2002**, *124*, 9394.
[20] J. Genzer, K. Efimenko, *Science* **2000**, *290*, 2130.